Preparation and bactericidal property of MgO nanoparticles on γ-Al_2O_3

YAN-JUN LIN, DIAN-QING LI, GE WANG, LEI HUANG, XUE DUAN*
Key Laboratory of Science and Technology of Controllable Chemical Reactions, Ministry of Education, Beijing University of Chemical Technology, Beijing 100029, People's Republic of China
E-mail: duanx@mail.buct.edu.cn

After being impregnated in the solution containing $Mg(NO_3)_2{\cdot}6H_2O$, γ-Al_2O_3 was dried and calcined at 500 °C which results in the production of a bactericide, highly dispersed MgO loaded on the surface of γ-Al_2O_3. The threshold value of the monolayer dispersion of MgO on γ-Al_2O_3 is 14.97%, and MgO crystal formed when the load amount beyond this value. The samples with different load amount were characterized by X-ray Diffraction (XRD), Low-temperature N_2 adsorption-desorption, Inductively Coupled Plasma (ICP) and High Resolution Scan Electronic Microscope (SEM). The results showed that these MgO microcrystals are highly dispersed and have regular size in the range of 4 to 10.8 nm. The specific surface, pore volume and pore size of the sample decreases with the increase of load amount. It is demonstrated that γ-Al_2O_3 with highly dispersed MgO on the surface is efficient bactericide, and the one with 20% load amount of MgO can kill more than 99% bacteria and spore cells.

1. Introduction

It is known that certain formulation of nano-scale powders possess bactericidal properties [1]. Examples include widely used TiO_2 and compounds of silver, copper or zinc. P. K. Stoimenov and his co-workers [2] have discovered that MgO particles with the crystal size less than 10 nm exhibit high bactericidal activity since their high surface, plenty of defects and positive charges on surface direct in strong reciprocity with electronegative bacteria or spores. Nano-MgO has the unique ability to destructively adsorb different gases [3, 4], including chemical warfare agents and surrogates [5, 6]. Another advantage of nano-MgO is that it exhibits good bactericidal activity under normal condition comparing with TiO_2 which has to be used under adscititious conditions like UV-light illumination [5]. Besides, Mg has more and cheap resource than other metals. Therefore it is desirable to develop a novel supported solid bactericidal agent, highly dispersed MgO with the particles size under 10 nm, which may have broad promising applications. Furthermore, supported nano-MgO is necessary since otherwise it is difficult to separate and recover nano-MgO after being used due to the very small size.

Considering the monolayer dispersion property of some metal oxides on porous supports [7, 8], in this study MgO is loaded onto the surface of γ-Al_2O_3 support and microcrystals of MgO at about 10 nm is obtained when the load amount is more than the monolayer dispersion threshold. Bacteriological test confirmed that the supported nano-MgO exhibits high activity against bacteria and spores.

2. Experimental section

2.1. Chemicals

$Mg(NO_3)_2{\cdot}6H_2O$ was of A.R. grade from Beijing Chemical Reagent Company. The strip-shaped support of γ-Al_2O_3 was obtained from Tianjin Institute of Chemical Industry. Mn_2O_3 was prepared by ourselves [7] with purity ≥99% (wt%) for the determination of the content of MgO crystals. Bacillus subtilis Var. niger (spore, ATCC9372) and Staphylococcus aureus (bacterium, ATCC6538) were purchased from China Academy of Medical Defence Science in form of slice packages, which have the bacteria number of 10^6 cfu/piece(colony forming units) and spore number of 70 cfu/piece.

2.2. Sample preparation

γ-Al_2O_3 support was milled and the powders with the size between 42.3 mm and 31.8 mm were collected, followed by calcination under 550 °C for 4 h. A certain amount of $Mg(NO_3)_2{\cdot}6H_2O$ based on the specific load amount of MgO was dissolved in 60 ml distilled water to form impregnation solution. About 10 g γ-Al_2O_3 was added into this solution, then the system was heated into 100 °C under stirring to vaporize the water among γ-Al_2O_3grains. The resulted product was dried at 120 °C

*Author to whom all correspondence should be addressed.

until no weight loss, followed by calcination at 500 °C for 12 h to produce MgO/γ-Al_2O_3 bactericidal agent with different load amount.

Nano-MgO is prepared according to a reported patent [9]. The dropwise addition of NaOH (OH^-/$Mg^{2+} = 2.0$) solution (5.0 mol/L) to $MgCl_2$ solution (1.0 mol/L) with agitating results in the formation of white emulsion. After the addition of NH_4HCO_3 ($HCO_3^-/Mg^{2+} = 1.5$) solution, the system is heated at 60 °C for 0.5 h. The resultant is cooled to room temperature and washed until no Cl^- is detected. The residual solid is dried under 70 °C for 3 h and calcined under 550 °C for 1 h to obtain nano-MgO powder.

2.3. Characterization

Powder XRD patterns were recorded on a Shimadzu XRD-6000 X-ray powder diffractometer using Cu K_α radiation between 10° and 70°. The scan speeds were 5°/min to analyze the phase type and 10°/min to measure the content of phase. Low-temperature N_2 adsorption-desorption isotherm was carried out using a Quantachrome Autosorb-1 system. The pore diameter distribution and pore volumes were calculated using the BJH method based on the desorption isotherm, and the surface area was calculated using the BET method based on the adsorption isotherm. The element content of samples was measured by JY-ULTIMA Inductively Coupled Plasma. High Resolution Scan Electronic Microscope (SEM) pictures were recorded by HITACHI S-4300 instrument.

2.4. Bacteriological test

A solution containing spores or bacteria was prepared by dissolving the slice into 5 ml physiological sodium chloride water. One tenth of this solution was fully contacted with 0.5 g MgO/γ-Al_2O_3 for 24 h. The mixture was filtered and the liquid phase was cultured for 48 h. After counting the alive number of spores or bacterium, the bactericidal efficiency was calculated according to the following formula:

$$\text{bactericidal efficiency (\%)} = \frac{\text{alive number in reference group} - \text{alive number in experiment group}}{\text{alive number in reference group}} \times 100\%.$$

3. Results and discussion

3.1. Dispersion characteristic of MgO on γ-Al_2O_3 and its monolayer threshold value

In each system the amount of γ-Al_2O_3 was fixed to be about 10 g and impregnated into the solution containing different amount of $Mg(NO_3)_2{\cdot}6H_2O$. The MgO content of each sample was 10.72, 13.28, 15.24, 17.32, 18.29, 19.06, 22.21 and 24.88%, respectively. As shown in Fig. 1, only characteristic diffraction peaks of γ-Al_2O_3 are observed when the load amount of MgO on γ-Al_2O_3 is too low. The diffraction peaks of MgO appear when the content of MgO exceeds a certain amount, and the intensity of the peaks increases with the load amount of MgO. This indicates that MgO disperses on γ-Al_2O_3 support in the monolayer way and the content of MgO has a maximum similar to other oxides [10]. When the load amount exceeds this limit, MgO crystal phase appears.

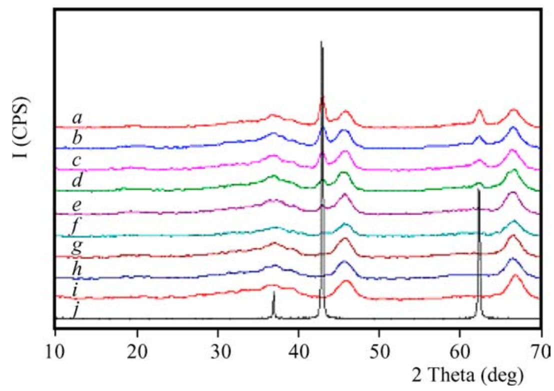

Figure 1 XRD patterns of MgO/γ-Al_2O_3 with MgO load of (a) 24.88%, (b) 22.21%, (c) 19.06%, (d) 18.29%, (e) 17.32%, (f) 15.24%, (g) 13.28% and (h) 10.72% as well as (i) γ-Al_2O_3 and (j) MgO.

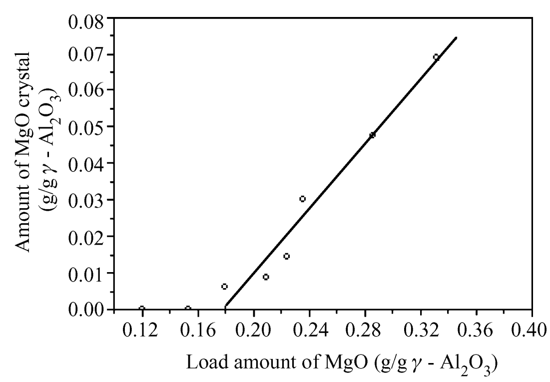

Figure 2 Correlation of MgO crystal amount with total MgO load.

The (200) peak of MgO ($2\theta = 42.908°$) and the (222) peak of Mn_2O_3 ($2\theta = 32.9°$) as reference to were chosen in order to determine the phase content of MgO in the mixture according to reported method proposed by F.H. Chung [11]. Fig. 2 illustrates the correlation of MgO crystal amount with MgO load for the samples calcined at 500 °C. When the load amount of MgO is rather low, there is no MgO phase and the experimental data site on the abscissa axis. With the load amount of MgO exceeds the monolayer threshold value, the experimental data increase according to a certain slope. The cross of the slope line and the abscissa axis represents the threshold value, which is 14.97% (wt%).

3.2. Pore character of MgO/γ-Al_2O_3 and the dispersion of MgO

In order to prepare MgO/γ-Al_2O_3 bactericides three batches are synthesized, in which the load amounts of MgO on γ-Al_2O_3 were accurately controlled at 15, 20 and 25%, respectively. As shown in Fig. 3, when the load amount is at 15% which is near the threshold, there is no diffraction peak of MgO. While the characteristic diffraction patterns of MgO are observed on the samples containing 20 and 25% MgO load, and the 25% one exhibits the highest intensity. The calculated average crystal size of MgO whose load amount at 20 and 25% was 10.6 and 10.8 nm, respectively, by Scherrer

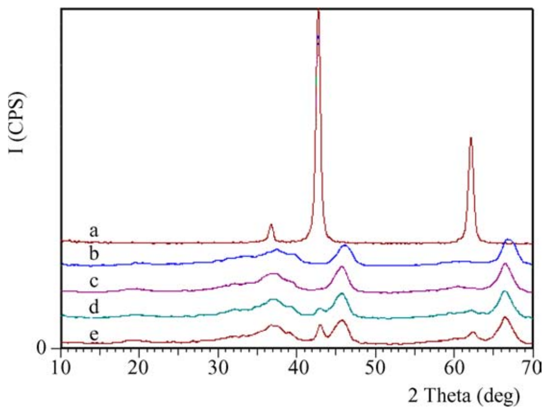

Figure 3 XRD patterns of (a) MgO, (b) γ-Al_2O_3 and MgO/γ-Al_2O_3 with MgO load of (c) 15%, (d) 20% and (e) 25%.

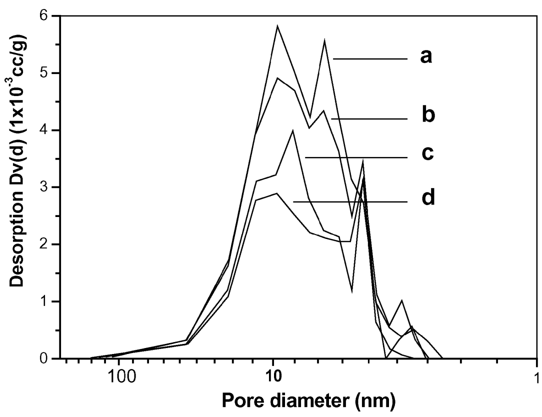

Figure 4 Pore size distribution of (a) γ-Al_2O_3 and MgO/γ-Al_2O_3 with MgO load of (b) 15%, (c) 20% and (d) 25%.

Equation [12]. This indicates that MgO spontaneously disperses on the surface of γ-Al_2O_3 to form MgO microcrystals when its load amount exceeds the threshold.

The results of the specific surface and pore volume are listed in Table I and the distribution of pore diameter of supported samples and γ-Al_2O_3support as well are shown in Fig. 4. Apparently MgO tends to overlay the whole surface of γ-Al_2O_3 in monolayer way when its load amount is below the threshold. The variety of MgO content has little effect on the specific surface, pore volume and pore size of the support before MgO can overlay the whole surface of γ-Al_2O_3. When the load amount of MgO exceeds the threshold, microcrystals of MgO under 10 nm also appear in the pores and outer surface of the support, and in addition these microcrystals which have similar size of support pores will block pores however. Therefore, the surface, pore volume and the pores size distribution of these samples change remarkably as the load amount increases from 15 to 20%, while little change after the load amount beyond 20%. This also indicates that more load MgO results in more formation of microcrystals.

TABLE I BET measurement results of MgO/γ-Al_2O_3 with different MgO load

Sample	Surface area (m^2/g)	Pore volume (cm^3/g)
γ-Al_2O_3	213.5	0.7138
15%MgO/γ-Al_2O_3	182.4	0.6590
20%MgO/γ-Al_2O_3	130.8	0.4945
25%MgO/γ-Al_2O_3	123.7	0.4522

Fig. 5 shows the High Resolution SEM of γ-Al_2O_3 support and MgO/γ-Al_2O_3 bactericides containing different load amount of MgO. Fig. 5(a) exhibits that γ-Al_2O_3 is formed by piling up many particles with similar size and the gaps of these particles are the source of its pores [13]. The pore edges of γ-Al_2O_3 become lee sharp and its surface becomes smoother in the function of monolayer dispersion and fill-up when the load amount of MgO is less than or equal to the threshold, and there is no microcrystal of MgO when the load amount is 15% as shown in Fig. 5(b). While it can be seen clearly from Fig. 5(c) that uniformly dispersed MgO microcrystals with size of 4–10 nm appears when the load amount achieves 20%. This means that MgO phase has formed when its load amount exceeds the

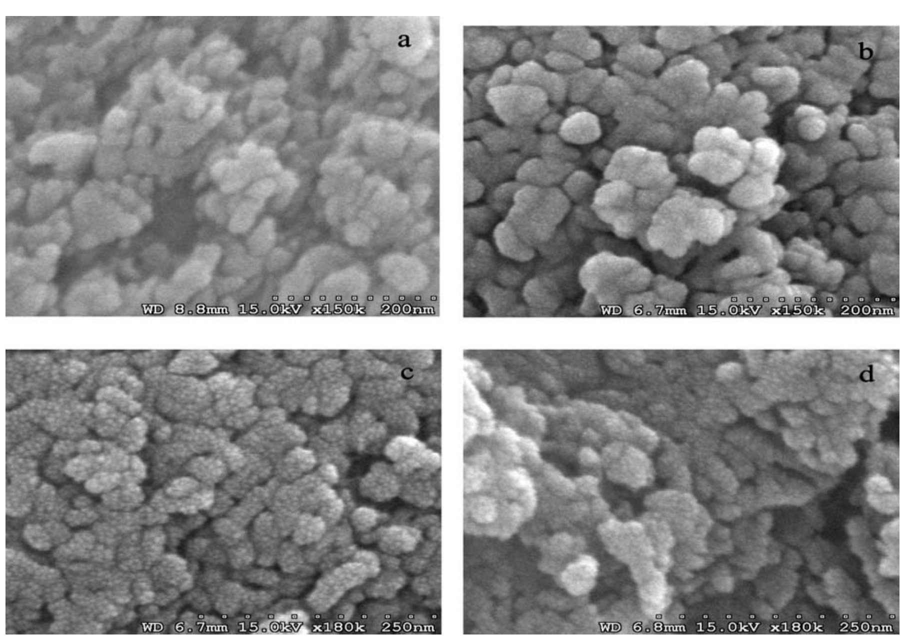

Figure 5 SEM images of (a) γ-Al_2O_3 and MgO/γ-Al_2O_3 with MgO load of (b) 15%, (c) 20% and (d) 25%.

TABLE II Sterilization results of $MgO/\gamma-Al_2O_3$ with different load of MgO

		Spore		Bacteria	
Load of MgO (%)	Average particle size of MgO (nm)	Residual number (cfu)	Sterlization efficiency (%)	Residual number (cfu)	Bactericidal efficiency (%)
15	0	7	0	too many	0
20	10.6	0	99.9	90400	99.23
25	10.8	2	71.4	107780	99.08

threshold in accordance with the results of XRD. As shown in Fig. 5(d), the number of MgO microcrystal has increased when the load amount reaches 25% while the particle size has little change compared with the sample of 20% load. These MgO microcrystals are connected and interfused with each other with the increase content of MgO.

3.3. Bactericidal efficiency of $MgO/\gamma-Al_2O_3$

After contacting with Bacillus subtilis Var. niger (spore, ATCC9372) and Staphylococcus aureus (bacterium, ATCC6538) for 24 h, the bactericidal efficiency of $MgO/\gamma-Al_2O_3$ with different MgO load amount is listed in Table II. The sample does not display bactericidal activity when the load amount of MgO is below the threshold since no MgO crystals formed. When MgO crystals are formed on the support, the samples exhibit excellent bactericidal efficiency since more than 99% of Staphylococcus aureus are killed. It is known that the bacteria size is about 1 μm, and as shown in Fig. 4, the pore diameter of $\gamma-Al_2O_3$ mainly distributes from 5 nm to 100 nm. Therefore the bactericidal activity mainly came from the nano-MgO microcrystals formed on outer surface of the support because bacteria and spores cannot enter these pores. Considering the residual bacteria number shown in Table II, the smaller the size of MgO, the better the bactericidal efficiency. This result is in good agreement with that of P.K. Stoimenov *et al.* [2]. Bacillus subtilis Var. niger is a kind of spore so that is more difficult to be killed comparing with Staphylococcus aureus that is a kind of bacteria. Therefore the survival rate of spore is affected strongly by the crystal size and distribution of MgO. As shown in Table II, the sterilization rate of sample rapidly decrease to 71.0% when the load amount of MgO is 25%.

4. Conclusions

$\gamma-Al_2O_3$ support was impregnated by a solution containing $Mg(NO_3)_2\cdot 6H_2O$ and calcined at 500 °C to form MgO, which displays monolayer dispersion character on the support. The threshold of monolayer dispersion for MgO is 14.97%. Microcrystals formed on the surface of $\gamma-Al_2O_3$ have the size of 4–10.8 nm, and they are isolated to each other once the load amount exceeds the threshold. The microcrystals on the inner surface of pores result in blockage of these pores and decrease the surface area, pore volume and pore diameter, while those on the exterior have main effect on the bactericidal action.

Bacillus subtilis Var. niger (spore, ATCC9372) and Staphylococcus aureus (bacterium, ATCC6538) are selected to test the bactericidal activity of the prepared samples. The results showed that there is no MgO crystal phase formed when the load amount below the monolayer threshold so that no bactericidal activity is observed. While the sample exhibits excellent bactericidal efficiency when the load amount is above the threshold. Because the bactericide of $MgO/\gamma-Al_2O_3$ which has 20% MgO has better bactericidal efficiency and can kill more than 99% bacteria since it has smaller size of MgO microcrystals comparing with other samples such as the one containing 25% MgO.

References

1. O. B. KOPER, J. S. KLABUNDE, G. L. MARCHIN, K. J. KLABUNDE, P. STOIMENOV and L. BOHRA, *Curr. Microb.* **44** (2002) 49.
2. P. K. STOIMENOV, ROSALYN L. KLINGER, GEORGE L. MARCHIN and KENNETH J. KLABUNDE, *Langmuir* **18** (2002) 667.
3. R. RICHARDS, W. LI, S. DECKER, C. DAVIDSON, O. KOPER, V. ZAIKOVSKI, A. VOLODIN, T. RIEKER and K. KLABUNDE, *J. Am. Chem. Soc.* **122** (2000) 4921.
4. E. LUCAS and K. KLABUNDE, *J. Nanostruct. Mater.* **12** (1999) 179.
5. S. KWAK, S. H. KIM and S. S. KIM, *Environ. Sci. Technol.* **35** (2001) 2388.
6. G. W. WAGNER, P. W. BARTRAM, O. KOPER and K. J. KLABUNDE, *J. Phys. Chem. B* **103** (1999) 3225.
7. RUI ZHANG, DIANQING LI, FAZHI ZHANG, DAVID G. EVANS and XUE DUAN, *Fine Chem.* **20** (2003) 74.
8. JIANG DE-EN, ZHAO BI-YING and XIE YOU-CHANG, *Appl. Catal. A: General* **19** (2001) 69.
9. DUAN XUE, LIN YANJUN and ZHANG HUI, *Chinese Patent*, CN02155467.6.
10. ZHANG YUFEN, XIE YOUCHANG, ZHANG YANG, ZHANG DELONG and TANG YOUQI, *Science in China (Series B)* **8** (1986) 805.
11. F. H. CHUNG, *Appl. Cryst.* **7** (1974) 526.
12. H. P. KLUG and L. E. ALEXANDER, in "X-Ray Diffraction For Polycrystalline and Amorphous Materials" (John Wiley & Sons, New York, 1974) p. 442.
13. ZHU HONGFA, in "Catalyst Supports" (Chemical Technology Publishing House, Beijing, 1980) p. 305.

Received 19 January and accepted 29 April 2004